The 5-Dehydro-*m*-xylylene Triradical and Its Nitrogen and Phosphorus Derivatives: Open-Shell Doublet versus Quartet Ground State

Hue Minh Thi Nguyen,[†,‡] **G. Gopakumar,**[†] **Jozef Peeters,**[†] **and Minh Tho Nguyen*,**[†]

Department of Chemistry, University of Leuven, Celestijnenlaan 200F, B-3001 Leuven, Belgium, and Faculty of Chemistry, University of Education, Hanoi, Vietnam

Received: May 24, 2004; In Final Form: July 25, 2004

Quantum chemical calculations have been applied to investigations of the electronic structure of the parent 5-dehydro-*m*-xylylene (DMX, or 5-dehydro-1,3-quinodimethane, C_8H_7) triradical containing a six-membered-ring radical coupled with two exocyclic CH_2 groups situated in the meta position, each containing an unpaired electron and its 4,6-dinitrogen (DMX-N) and 4,6-diphosphorus (DMX-P) derivatives. The purpose of the study is to determine the identity of their electronic ground states. Our results obtained using state-averaged complete active space self-consistent-field (CASSCF) followed by second-order multistate multiconfiguration perturbation theories MS-CASPT2 and MR-QDPT in conjunction with large ANO-L and the 6-311G(d,p) basis set reveal the following: (i) DMX has a three-open-shell ($\sigma^1\pi^1\pi^1$) doublet $^2B_2$ ground state with a $^4B_2$–$^2B_2$ energy gap in the range 1−3 kcal/mol, and (ii) the ground state of both DMX-N and DMX-P triradicals is also the doublet $^2B_2$ being below the $^4B_2$ state by 1 and 2 kcal/mol, respectively. In the triradicals considered, both doublet and quartet states are nearly degenerate but have a slight preference for the low-spin state, apparently violating Hund's rule. Protonation at C5 of DMX giving the $MX^{\bullet+}$ radical cation modifies the electronic landscape, the one-open-shell doublet $^2B_1$ being the $MX^{\bullet+}$ ground state. The electron affinities (EAs), ionization energies (IEs), and proton affinities (PAs) are computed for the triradicals. For DMX: EA = 1.1 eV, IE = 7.50 eV, and PA = 401 kcal/mol. For DMX-N: EA = 2.3 eV, IE = 8.20 eV, and PA = 233 kcal/mol. For DMX-P: EA = 4.5 eV, IE = 8.98 eV, and PA = 214 kcal/mol. Comparable data for the anions follows. PA = 401, 367, and 371 kcal/mol for DMX^-, $DMX-N^-$, and $DMX-P^-$, respectively.

1. Introduction

Reactive intermediates form a fascinating world, owing not only to their key role in chemical transformations, but also to their intrinsically bewildering nature and deceptively complicated electronic structure and molecular properties.[1] Of transient intermediates, diradicals in which two unpaired electrons occupy two nearly degenerate orbitals, and the partially filled orbitals reside on two different atomic centers, are relatively well characterized.[2] Derived from a two-electrons-in-two-orbitals distribution, the electronic ground state of a diradical could in general be a triplet or an open-shell or closed-shell singlet state.

Non-Kekulé hydrocarbon diradicals (Scheme 1) such as trimethylenemethane (TMM) and *m*-xylylene (MX) (also named *m*-benzoquinodimethane) exhibit a triplet ground state,[3] whereas tetramethyleneethane (TME) and tetramethylenebenzene (TMB) feature a singlet ground state.[4] When two open-shell centers are linked by a phenyl moiety such as in *p*-phenyl-bis-carbene (*p*-PhX, X = CH) and its nitrene (*p*-PhX, X = N) and phosphinidene (*p*-PhX, X = P) analogues, the open-shell singlet becomes also the ground state[5] (for the notations, cf. Scheme 1). However, in all these cases, the energy gaps between both multiplicity manifolds are small, amounting to only a few kilocalories per mole. In a sense, singlet ground-state diradicals

violate both the Aufbau principle and Hund's rule that govern the electron occupancy of molecular orbitals.

Recently, Slipchenko et al.[6] were able to generate, using mass spectrometric techniques, the gas-phase 5-dehydro-*m*-xylylene (DMX, Scheme 1), which is formally a hydrocarbon triradical (C_8H_7). Using quantum chemical calculations with a spin-flip technique SF-CCSD/6-311G(d,p),[7] these authors derived an energy gap of 3.7 kcal/mol (0.16 eV) in favor of the three-open-shell doublet $^2B_2$ state over the corresponding quartet $^4B_2$ state. The SF technique is based on coupled-cluster reference wave functions in which the single and double excitation operators involve the flip of the spin of one electron. Accordingly, the open-shell doublet state arises from an occupation of three unpaired electrons in three orbitals having comparable energy but different symmetry, $^2B_2$, $(a_1)^1(b_1)^1(a_2)^1$. While the a_1 orbital corresponds to an in-plane σ orbital at the C5 position, both b_1 and a_2 orbitals contain π components. Such a preference for low-spin structure could be understood by the fact that, in MX, where two ($\pi^1\pi^1$) electrons interact, a ferromagnetic triplet state is preferred. In DMX, the existence of unpaired σ and π electrons leads to a more dominant antiferromagnetic coupling.

Even though low-spin open-shell states often occur in transition-metal complexes, DMX represents a nice and rare example of a hydrocarbon triradical having a three-open-shell ($\sigma^1\pi^1\pi^1$) electron configuration and a doublet ground state.[8] Thus, with the emergence of low-spin states in a multispin configuration, Hund's rule is once more broken down![6]

* Corresponding author. E-mail: minh.nguyen@chem.kuleuven.ac.be. Fax: 32-16-32 7992.
† University of Leuven.
‡ University of Education.

SCHEME 1

TMM (Triplet)

MX (Triplet)

TME (Singlet)

TMB (Singlet)

p-PhX (Singlet)
(X=CH, N, P)

DMX
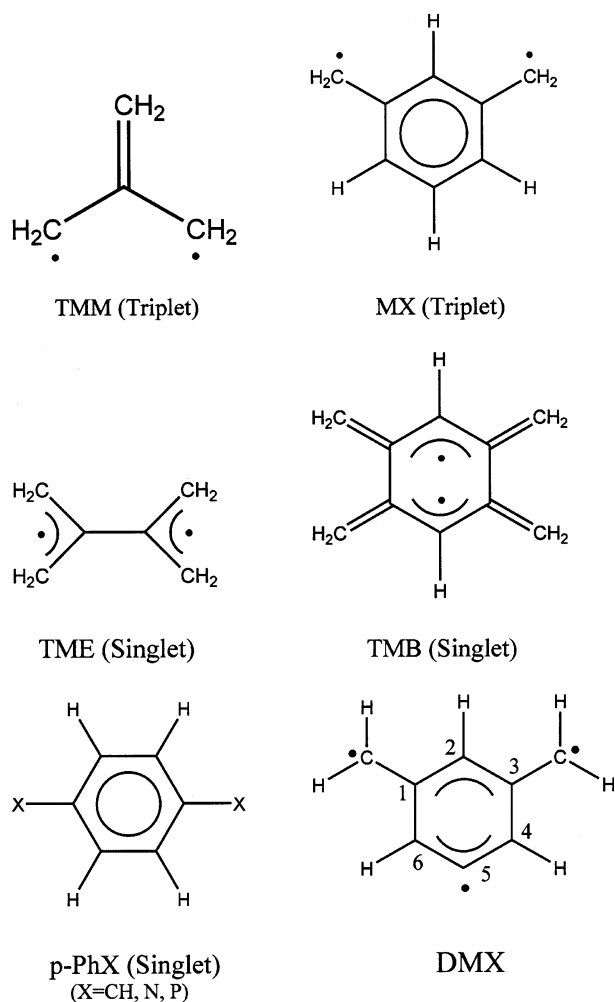
In ref 6, some useful thermochemical parameters were also derived from mass spectrometric measurements. A proton-transfer bracketing technique was set up for determining the basicity of anions, and a kinetic method was developed for determining the electron affinity of radicals. The electron affinity EA(DMX), the gas-phase acidity of the C5 position of MX (basicity of the DMX$^-$ anion, cf. Scheme 1 for atom numbering), and the bond dissociation energy BDE(C−H) of MX were thus evaluated experimentally.

In view of the novelty of the DMX electronic structure, which indeed represents another typical case of three-electrons-in-three-orbitals in an organic molecule,[8] and in an attempt to evaluate the reliability of different procedures for treating multiple-spin species,[7] we set out to investigate its electronic state by making use of appropriate quantum chemical methods. In considering also some associated heteroatom derivatives, a few relevant questions could be posed: (i) What is the identity of the DMX ground state and the extent of the quartet−doublet energy gap? (ii) Upon protonation of DMX at the C5 position, giving rise to a MX$^{\bullet+}$ radical cation, does such quartet−doublet duality remain unchanged? (iii) Following electron attachment to DMX, does the DMX$^-$ have the same electronic structure as the neutral MX? (iv) What kind of modifications in the electronic state could we expect when the two CH groups in C4 and C6 of MX are replaced by two nitrogen atoms? (v) And finally, could the phosphorus atom, which also has an electron pair but a lower electronegativity than nitrogen (2.19 for P and 3.04 for N), produce similar effects? Overall, we have consid-

SCHEME 2

MX-a (a=CH, N, P)

DMX-a (a=CH, N, P)

DMX-a$^-$ (a= CH, N, P)

MX-a$^{\bullet+}$ (a= CH, N, P)
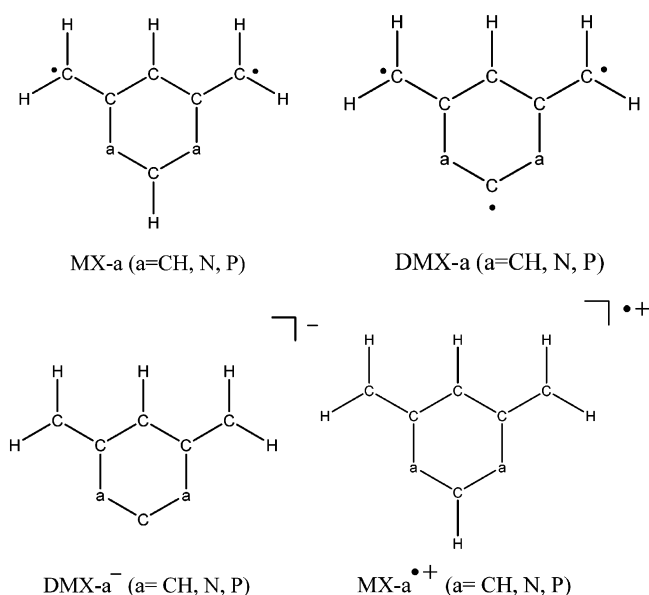
ered the electronic structure and energies of the species listed in Scheme 2 where **a** stands for CH, N, and P.

2. Methods of Calculation

The calculation of energies of quasidegenerate electronic states has long been a challenge for computational quantum chemistry. The possibility for accurate determination of such states in molecular systems has now been realized through the development of improved quantum chemical techniques. The multiconfigurational self-consistent-field (MCSCF) method and, in particular, the complete active space self-consistent-field method (CASSCF)[9] usually correct for nondynamical or quasi-degenerate correlation effects within the active space. Because, in an MCSCF wave function, many of the valence electrons have been treated as filled closed-shell orbitals with no recovery of correlation energy whereas active electrons have partial recovery of correlation, this approach cannot account for the additional correlation referred to as dynamical correlation. The latter mainly arises from the excitation of the active electrons or inert valence electrons into the virtual orbitals. To recover dynamic correlation energy, the CASPT2[10] and MRMP2[11] methods have been applied.

It has been known that, when applying separately a perturbative treatment to MCSCF states with very close energies, the states ordering could be reversed and the results become unphysical if the states are of the same symmetry, as in most cases, a root flipping occurs or the perturbation series diverges because of the existence of intruder states.[12] The latter, which arises from the near-singularities caused by very small or vanishing energy denominators of the corresponding perturbation expansions, often occurs because high-lying states within the complete active space frequently have zeroth-order energies that are quasidegenerate with zeroth-order states in the orthogonal space. The orthogonal space states that are quasidegenerate with reference space states and are disrupting the perturbative convergence are called intruder states,[12] and it is believed that it often occurs in MRMP treatment when the reference state is a high-lying state and a basis set with diffuse functions is used. Such problems could be circumvented by the application of a quasidegenerate perturbation theory (QDPT) where a small energy denominator shift value is used.[13] In this context, the multistate MS-CASPT2 method[14] is an extension and improve-
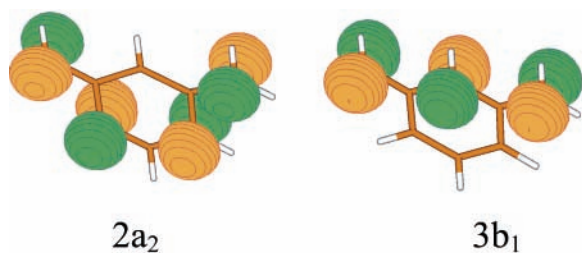
Figure 1. Shape of two highest-lying orbitals of MX biradical (C_8H_8) whose occupancy determines the electronic state. Both are natural orbitals obtained from an optimized CASSCF wave function.
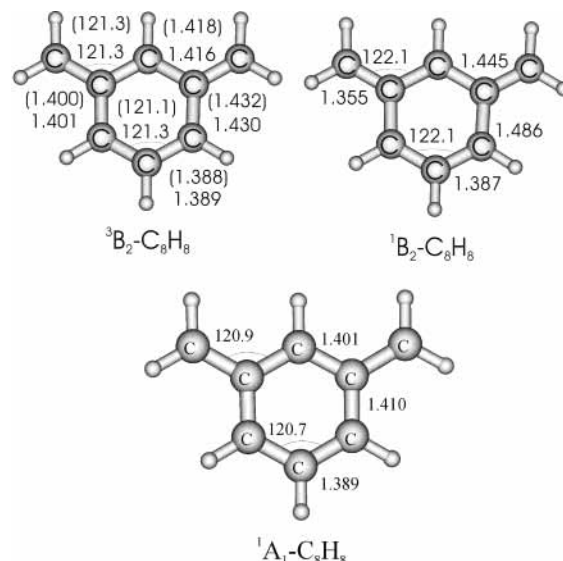

Figure 2. Selected CASSCF(10,9)/ANO-L and B3LYP/6-311++G-(3df,2p) (values in parentheses) geometrical parameters of MX biradical considered in three lower-lying electronic states. Bond distances are given in angstroms and bond angles in degrees.

SCHEME 3

ment of the CASPT2 method and considers the coupling of a number of lower-lying CASPT2 states of the same symmetry. The multistate multiconfigurational quasidegenerate perturbation (MCQDPT) method[15] is another comparable approach, in which the Van Vleck perturbation theory is applied. The effective Hamiltonian in MCQDPT contains off-diagonal corrections as well as single-state corrections to the diagonal terms and yields improved total energies at second order for all states included in the model space simultaneously. Therefore, the main advantage of a multistate perturbation approach is a simultaneous determination of the energies of several states of interest including degenerate or quasidegenerate states.

In this work, the lowest-lying valence electronic states of the radicals considered were investigated employing both the MS-CASPT2 and MCQDPT methods. Although for MS-CASPT2/ CASSCF calculations a large atomic natural orbitals (ANO) basis set has been chosen, for MCQDPT/CASSCF computations, the 6-311G(d,p) basis set has been used. For high-spin triplet and quartet states that are in particular not severely affected by orbital degeneracy and can thus be represented by single-determinantal Hartree–Fock wave functions, density functional theory (DFT) calculations using the B3LYP hybrid functional[16] were also performed. All calculations were carried out using the *Gaussian 98,*[17] *GAMESS*,[18] and *Molcas*[19] suites of programs.

Geometrical parameters of the species considered were initially optimized using both HF and B3LYP methods in conjunction with the dp-polarization plus diffuse functions 6-311++G(3df,2p) basis set and within the unrestricted formalism (UHF, UB3LYP). The character of the structures located was determined by harmonic vibrational frequencies calculated at the same level. Unfortunately, we were not able to carry out vibrational frequency computations at the CASSCF level; therefore, the zero-point energy (ZPE) corrections to the relative energies could only be determined for structures that can be characterized at the B3LYP level. Unless otherwise noted, bond distances are given in angstroms and bond angles in degrees.

3. Results and Discussion

A. *meta*-Xylene Biradical (C_8H_8) and Its Ions. Before examining the triradicals, let us consider for a preliminary calibration the *meta*-xylene (C_8H_8, MX, cf. Scheme 1), for which some experimental and theoretical studies are available.[2,3] MX is a formal C_8H_8 hydrocarbon biradical whose C_{2v} point group symmetry leads to the two highest-energy molecular orbitals ($2a_2$) and ($3b_1$) displayed in Figure 1. These are natural orbitals obtained from an optimized CASSCF computation. Variable occupancy of these two MOs by two available electrons gives rise to the triplet $^3B_2$, open-shell singlet $^1B_2$, and closed-shell singlet $^1A_1$ electronic states. To simplify the presentation, the shape of the nine MOs selected for the active space in CASSCF-(10,9) calculations including one a_1, three a_2 and five b_1 orbitals are illustrated in Figure 1S of the Supporting Information.
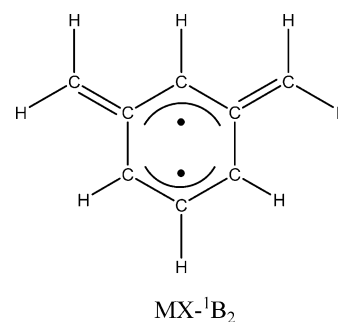
Although a_1 corresponds to a σ orbital, the remaining orbitals are of π character. The b_2 orbitals are not included because they do not show significant contributions. Although for the neutral biradical, an (8,8) active space is sufficient to describe the nondynamical correlation, we have rather chosen a (10,9) space because of the fact that, in the $C_8H_8^{\bullet+}$ cation, an electron could be removed from the a_1 orbital, implying a set of 9 correlated electrons. For the sake of consistency, the (10,9) active space has been selected for both neutral and ionized systems.

Selected geometrical parameters of these states, optimized using both CASSCF(10,9)/ANO and UB3LYP/6-311++G-(3df,2p) methods, are given in Figure 2. The geometries derived by both MO and DFT methods for the triplet $^3B_2$ are nearly identical. While the parameters of the closed-shell singlet state $^1A_1$ are close to those of the triplet counterpart, the values for the open-shell singlet $^1B_2$ differ significantly. In the $^1B_2$ state, the exocyclic C–C distance is shorter (1.355 Å versus 1.401 Å) and thus is close to a double bond, whereas the two adjacent endocyclic C–C bonds become longer (1.445 Å versus 1.416 Å). This confirms a shift of the radical centers from outside into the six-membered ring, and they are rather delocalized within the ring in MX ($^1B_2$) as depicted in Scheme 3. Details of the MS-CASPT2 and MCQDPT computations using CASS-CF optimized geometries are summarized in Table 1. Note that the values given are derived without ZPE corrections.

In agreement with previous results[3] derived from a photo-electron (PES) study and generalized valence bond (GVB) calculations of the *meta*-xylylene radical anion (MX[•−]), we have

TABLE 1: Calculated Results Using MS-CASPT2/ANO-L, MRMP2/6-311G(d,p) and MCQDPT/6-311G(d,p) for MX (C$_8$H$_8$) and Its Radical Cation (C$_8$H$_8$)$^{\bullet+}$

state	a$_1$	a$_2$	b$_1$	weight[c]	MS-CASPT2	MRMP2	MCQDPT
					total energy[b] (au) (relative energy in kcal/mol)		
MX Molecule							
^{3}B$_2$	2	2u0	22u00	0.810	−308.767 64	−308.719 02	−308.711 77
	2	udu	22u00	0.023	(0)	(0)	(0)
	2	2u0	2du0u	0.019			
	2	2u0	2uu0d	0.013			
	2	uuu	22d00	0.010			
^{1}A$_1$	2	220	22000	0.441	−308.749 58	−308.700 86	−308.697 34
	2	200	22200	0.429	(11.3)	(11.4)	(9.1)
^{1}B$_2$	2	2u0	22d00	0.832	−308.729 56		
	2	u20	22d00	0.018	(23.9)		
	2	20u	22d00	0.013			
	2	2u0	d2ud0	0.011			
MX$^{\bullet+}$ Molecule							
^{2}B$_1$	2	200	22u00	0.801	−308.503 04	−308.457 13	−308.458 62
	2	uu0	22d00	0.053	(0)	(0)	(0)
	2	020	22u00	0.016			
	2	220	2u000	0.011			
^{2}A$_2$	2	2u0	22000	0.794	−308.493 17	−308.443 96	−308.445 09
	2	u00	22200	0.027	(6.2)	(8.3)	(8.5)
	2	0u0	22200	0.018			
	2	2u0	2d0u0	0.015			
	2	2u0	2du00	0.010			
^{4}A$_2$	2	2u0	2uu00	0.874	−308.429 64		
	2	udu	2uu00	0.015	(46.1)		

[a] The active space includes 9 orbitals: 1 × a$_1$, 3 × a$_2$, 5 × b$_1$. u stands for spin up (α), and d stands for down spin (β); 2 stands for doubly occupied. No b$_2$ orbitals are considered. [b] On the basis of CASSCF/ANO-L-optimized geometries given in Figures 2 and 3. [c] CI coefficients are obtained from CASSCF wave functions.

found that the neutral MX is characterized by a triplet ^{3}B$_2$ ground state. The closed-shell singlet ^{1}A$_1$ turns out to be lower in energy than the open-shell singlet ^{1}B$_2$, which is centered at 23 kcal/mol above the triplet.

In regard to the MX singlet−triplet separation, either CASSCF or MCSCF computations result in a gap of 14 kcal/mol. Both the MS-CASPT2 and MRMP2 methods provide a similar gap of approximately 11 kcal/mol, whereas MCQDPT yields a smaller value of 9 kcal/mol. The difference between MS-CASPT2 and intruder-states-free MCQDPT methods likely arises from the basis sets employed. In this regard, the MS-CASPT2/ANO-L value of 11 kcal/mol could be considered as a better estimate. Including a ZPE correction of 1 kcal/mol, the calculated energy gap amounts to 10 kcal/mol. In any case, when taking an expected error of ±1 kcal/mol into consideration, all of the multistate computed values can be compared with the experimental PES results of 9.6 ± 0.2 kcal/mol derived for the ^{1}A$_1$−^{3}B$_2$ gap of MX and an upper bound of 21.5 kcal/mol for its ^{1}B$_2$−^{3}B$_2$ gap.[3] Note that the density functional B3LYP method provides a substantially larger ^{1}A$_1$−^{3}B$_2$ gap of 26 kcal/mol, and this approach should be used with much caution in evaluating the energy separations of this type of compound. The difficulty of DFT methods in evaluating the singlet−triplet gaps, from a general point of view, has formally been proven.[20]

In the experimental study,[3] an electron affinity EA(MX) = 0.919 ± 0.008 eV was also derived. B3LYP computations confirmed that, of the two possible doublet states of MX$^{\bullet-}$ derived from MX by addition of an electron to one of the two orbitals 2a$_2$ (giving ^{2}B$_1$) and 3b$_1$ (giving ^{2}A$_2$), the ^{2}B$_1$ state is found to be the ground state. The adiabatic electron affinity of MX is calculated to be 0.90 eV at the UB3LYP/6-311++G-
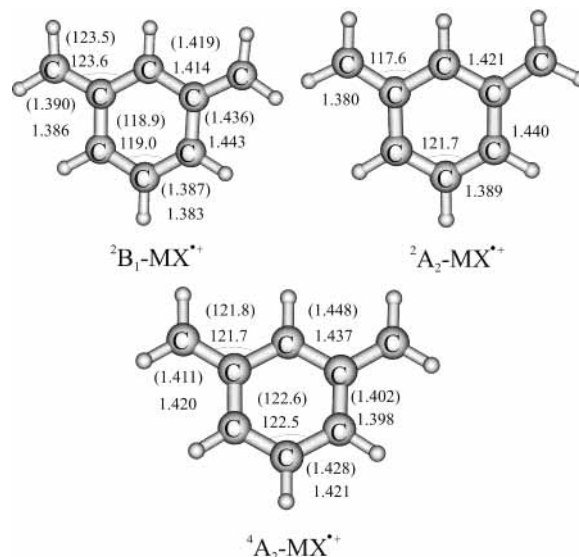

Figure 3. Selected CASSCF(9,9)/ANO-L and B3LYP/6-311++G-(3df,2p) (values in parentheses) geometrical parameters of MX$^{\bullet+}$ radical cation (C$_8$H$_8$$^{\bullet+}$) considered in three lower-lying electronic states. Bond distances are given in angstroms and bond angles in degrees.

(3df,2p) + ZPE level, which is quite close to the PES value mentioned already.

After removal of an electron from the triplet MX, different electronic states of the resulting MX$^{\bullet+}$ radical cation could be formed. Employing the same set of nine orbitals given in Supporting Information Figure 1S, we have carried out MS-CASPT2(9,9)/ANO-L and MCQDPT/6-311G(d,p) computations on MX$^{\bullet+}$ whose details are also summarized in Table 1 and thereby identified three low-lying states. Selected geometrical parameters of these states determined using CASSCF and B3LYP are given in Figure 3. Where available, the B3LYP values are quite close to the CASSCF counterparts. Geometrical parameters differ only slightly in going from one state to the other. This indicates that the unpaired electron is rather delocalized over the whole molecular skeleton.

The doublet ^{2}B$_1$ state is found to constitute the ground state of MX$^{\bullet+}$, followed by the ^{2}A$_2$ state which is higher in energy, amounting to approximately 6 kcal/mol by MS-CASPT2 but approximately 8.5 kcal/mol by MCQDPT. It seems reasonable to propose an estimate of 7 ± 1 kcal/mol for the ^{2}A$_2$−^{2}B$_1$ gap. The lowest-lying quartet ^{4}A$_2$ state is found to lie 46 kcal/mol higher than the ground state (MS-CASPT2 value). After we have taken ZPE corrections evaluated using B3LYP calculations into account, the ^{4}A$_2$−^{2}B$_1$ gap of MX$^{\bullet+}$ becomes 44 kcal/mol.

The adiabatic ionization energy of IE$_a$(MX), taken as the energy difference between the ^{3}B$_2$(MX) and the ^{2}B$_1$(MX$^{\bullet+}$), is calculated at 7.20 eV by MS-CASPT2, 7.12 eV by MRMP2, 6.90 eV by MCQDPT, and 7.37 eV by UB3LYP. It is well-known that the IE$_a$'s are usually underestimated by up to 0.3 eV by high-level MO methods and up to 0.2 eV by DFT methods;[21] we would therefore take an upper-bound value of all these calculations as a realistic estimate for this quantity. This leads to an ionization energy IE$_a$(MX) = 7.5 ± 0.2 eV.

B. 5-Dehydro-*meta*-xylylene (C$_8$H$_7$) Triradical. Having established the validity of our approach for the MX biradical, we now consider the DMX triradical which is derived from MX following dehydrogenation at the C5 position. For the sake of consistency, we have employed a similar set of MOs in the active space for CASSCF(9,9)/ANO-L calculations. The shapes of the relevant nine orbitals with symmetries a$_1$ (one), a$_2$ (three), and b$_1$ (five) are illustrated in Figure 4. Again, no b$_2$ orbitals

Xylylene Triradical and Derivatives
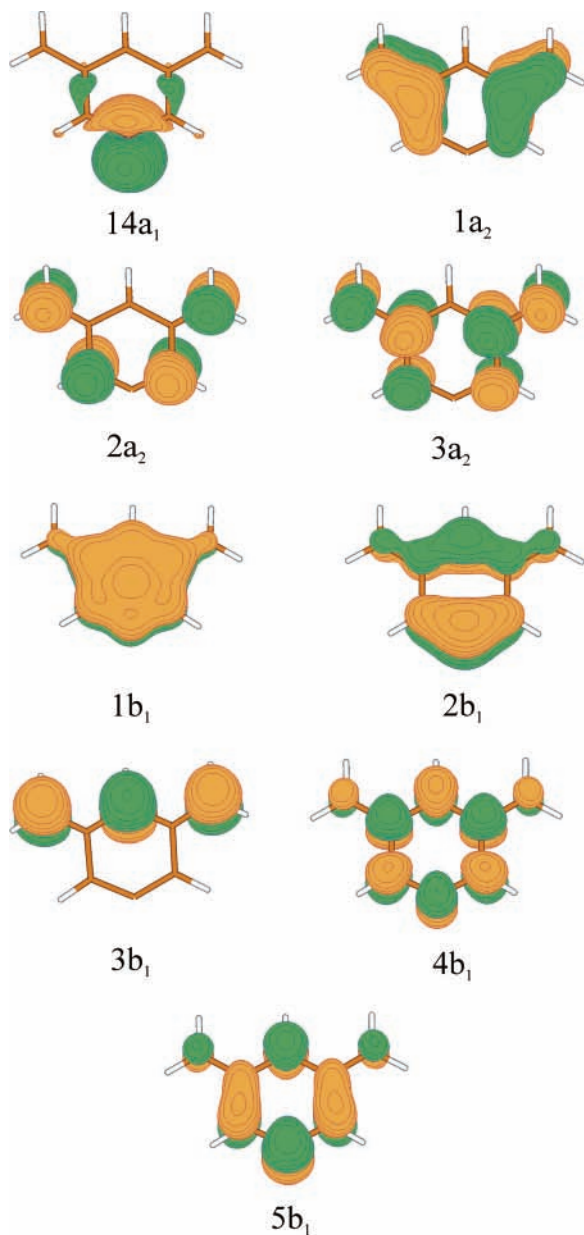
J. Phys. Chem. A, Vol. 108, No. 40, 2004 **8415**

Figure 4. Shape of a set of natural orbitals included in the active space of CASSCF(9,9) computations for the DMX triradical and its ions.

TABLE 2: Calculated Results Using MS-CASPT2/ANO-L, MRMP2/6-311G(d,p), and MCQDPT/6-311G(d,p) for C_8H_7

	main orbital configurations[a]				total energy[b] (au) (relative energy in kcal/mol)		
state	a_1	a_2	b_1	weight[c]	MS-CASPT2	MRMP2	MCQDPT
					DMX Molecule		
$^2B_2$	u	2d0	22u00	0.616	−308.087 22	−308.045 16	−308.042 14
	u	2u0	22d00	0.187	(0)	(0)	(0)
	u	2u0	2du0d	0.022			
	u	2d0	2ud0u	0.017			
	u	dud	22u00	0.015			
	u	udu	22d00	0.014			
$^4B_2$	u	2u0	22u00	0.817	−308.084 19	−308.041 29	−308.037 99
	u	2d0	2uu0u	0.018	(1.9)	(2.4)	(2.6)
	u	udu	22u00	0.016			
	u	uuu	22d00	0.012			

[a] The active space includes 9 orbitals: $1 \times a_1$, $3 \times a_2$, $5 \times b_1$. u stands for spin up (α), and d stands for down spin (β); 2 stands for doubly occupied. No b_2 orbitals are considered. [b] On the basis of CASSCF/ANO-L-optimized geometries given in Figure 5. [c] CI coefficients are obtained from CASSCF wave functions.
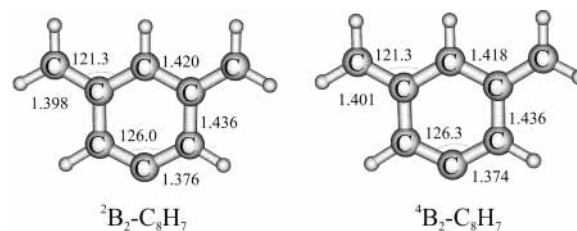

Figure 5. Selected CASSCF(9,9)/ANO-L geometrical parameters of DMX triradical (C_8H_7) in lowest-lying doublet and quartet electronic states. Bond distances are given in angstroms and bond angles in degrees.

are incorporated in the active space (Supporting Information Figure 2S). In general, the shapes of these MOs do not differ significantly from those of MX (Supporting Information Figure 1S).

The orbital configurations having important contributions to the wave functions of the lowest-lying doublet and quartet states of DMX are given in Table 2, along with the energies calculated using different schemes. As mentioned above, each B_2 state features a distribution of three electrons occupying three nonbonding orbitals, namely $(a_1)^1(b_1)^1(a_2)^1$, leading to three open shells. The other doublet states have only one open-shell orbital, and the weight of the main reference amounts to approximately 0.75.

Geometrical parameters of both $^2B_2$ and $^4B_2$ states are summarized in Figure 5. Because their geometries are quite close to each other, it can be expected that their ZPEs are also of comparable magnitude.

CASSCF results indicate the $^2B_2$ state as the lower-lying state at 3.3 kcal/mol below the $^4B_2$ counterpart. The dominant configuration is characterized by weights of 0.62 and 0.19,

followed by several configurations with coefficients smaller than 0.14. As seen in Table 2, the electrons in both orbitals $14a_1$ and $2a_2$ are coupled to each other with α and β spins, and the doublet multiplicity arises mainly from the singly occupied electron (α spin) in the $3b_1$ orbital (cf. Figure 4). The latter is a π orbital with lobes on the C2 and exocylic C atoms. The leading configuration in the $^4B_2$ state has a contribution of 0.82 to the total wave function. The MS-CASPT2 approach provides a smaller quartet−doublet gap of 1.9 kcal/mol, whereas the state-specific MRMP2 and MCQDPT calculations place the quartet state 2.4 kcal/mol above its doublet counterpart. Again, the small difference between the MS-CASPT2 and MCQDPT values likely results from a difference in the one-electron functions employed. The present values are slightly smaller than the 3.7 kcal/mol derived in earlier SF-CCSD/6-311G(d,p) computations.[6] Overall, calculated results tend to suggest a small energy separation, with a marginal preference for the low-spin state. In view of the fact that the ZPE contributions are small and the larger ANO-L basis set was used in the MS-CASPT2 calculations, we would suggest a $^4B_2-{}^2B_2$ energy separation of 2.0 ± 1 kcal/mol for DMX.

The relative vertical locations of higher-lying doublet states of DMX are identified from MS-CASPT2/ANO-L calculations as follows (values in kcal/mol): X^2B_2 (0.0) < a^4B_2 (2.0) < $A1^2A_1$ (12.5) < $B2^2B_2$ (27.0) < $C1^2B_1$ (28.5) < $D1^2A_2$ (48.3). It is apparent that several lower-lying states of DMX emerge within a range 3.0 eV from the ground state.

To evaluate the electron affinity of DMX, we have also examined the anion DMX⁻. In contrast to the isoelectronic MX species, the latter anion exhibits a $^3B_1(DMX^-)$ $(a_1)^1(b_1)^1$ ground state, resulting from a filling of the a_2 orbital of DMX by the added electron. Calculated results suggest an electron binding

energy EA(DMX) $= 1.1$ eV, with an expected error of ± 0.2 eV, which is in good agreement with the experimental value of 1.08 ± 0.2 eV (24.9 ± 2.0 kcal/mol).[6] This value is slightly larger than the experimental electron affinity EA(MX) $= 0.919$ eV for the MX biradical.[3] Note that the other possible triplet state arising from the filling of the b_1 orbital yielding $^3A_2$(DMX$^-$) $(a_1)^1(a_2)^1$ is calculated to be marginally higher in energy, namely at 0.9 eV below DMX and thus only 0.2 eV above the ground state $^3B_1$.

The available total energies of the various species also allow the proton affinities (PAs) to be evaluated. For this quantity, the B3LYP/6-311++G(3df,2p) + ZPE level provides the most appropriate results. Accordingly, the proton affinity of the DMX$^-$ anion, as the energy difference between DMX$^-$($^3B_1$) and MX($^3B_2$), amounts to PA(DMX$^-$) $= 401.4$ kcal/mol, which agrees well with the experimental result of 401 ± 3 kcal/mol determined using the proton-transfer bracketing experiments[6] for DMX$^-$. Using the same level of theory, a proton affinity of the DMX triradical, which is the energy difference between DMX($^2B_2$) and MX$^{\bullet+}$($^2B_1$), could be evaluated, PA(DMX) $= 261$ kcal/mol, with a probable error of ± 3 kcal/mol. It is interesting to note here that the protonated form MX$^{\bullet+}$ (C$_8$H$_8^{\bullet+}$ radical cation) exhibits a completely different electronic landscape as compared with its neutral C$_8$H$_7$ DMX counterpart. The formation of an additional C−H bond results in a pure one-electron radical character for MX$^{\bullet+}$.

C. The Nitrogen and Phosphorus Triradicals. We now turn to the two derivatives of the triradical, in which both CH groups at the 4 and 6 position of the six-membered ring are replaced successively by two nitrogen atoms (noted as DMX-N, Scheme 2) and by two phosphorus atoms (DMX-P). Incorporation of N or P obviously introduces two lone pairs of electrons at each site. Combination of the corresponding atomic orbitals leads to a_1 and b_2 MOs. It is of interest to investigate whether the lone pair electrons of N or P have any significant correlation or interaction. Separate CASSCF state-averaged computations on the two lowest-lying states with and without N/P lone pairs show that the latter were mostly doubly occupied in CASSCF wave functions, with an occupation number larger than 1.97. The resulting energy gaps from the two CASSCF sets differ by approximately 0.3 kcal/mol. Because the energy gaps are also small, approximately 2 kcal/mol, a variation of 0.3 kcal/mol already represents 15% of the gap. Therefore, it seems reasonable to incorporate the lone pair orbitals. The active space used in CASSCF(13,11) calculations is now composed of two a_1, three a_2, one b_2, and five b_1 orbitals (Supporting Information Figure 3S), including two additional lone pair a_1 and b_2 orbitals. The relative importance of the latter could not be a priori determined; therefore, we have included both in the active space. We are well aware of the fact that a doubly occupied orbital with an occupancy number larger than 1.97 could introduce redundant rotations during the iterative process, between the closed and active shells.[22] Nevertheless, the CASSCF processes were well converged in this case.

Figure 6 displays only the shape of the three orbitals (a_1, b_1, and a_2) determining the electronic state of the DMX-N triradical. The orbitals used in the active space for DMX-P exhibit the same number, symmetry, and shape. Details of the MS-CASPT2 and MCQDPT calculations for both lowest-lying doublet and quartet states are listed in Table 3.

For the $^2B_2$ state, the CI coefficients indicate a large mixing of configurations, the largest being approximately 0.60 and 0.20. A coupling between the β spin of electrons in a_2 orbital and α spin of electrons in b_1 and a_1 orbitals leads to an open-shell
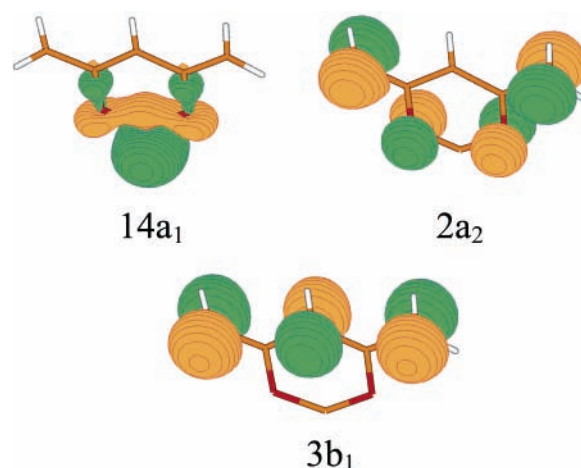

Figure 6. Shape of a set of natural orbitals included in the active space of CASSCF(13,11) computations for the DMX-N triradical.
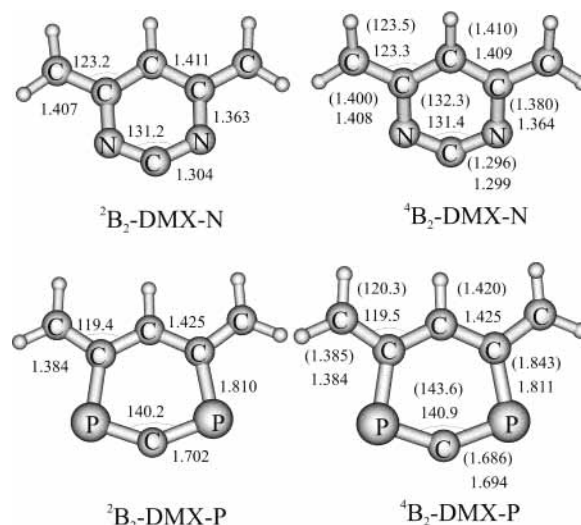

Figure 7. Selected CASSCF(13,11)/ANO-L and B3LYP/6-311++G-(3df,2p) (values in parentheses) geometrical parameters of DMX-N and DMX-P triradicals considered in lowest-lying doublet and quartet electronic states. Bond distances are given in angstroms and bond angles in degrees.

doublet π radical. For the $^4B_2$ state, the leading configuration has a contribution of 0.78 to the CASSCF wave function.

Selected geometrical parameters optimized using CASSCF-(13,11)/ANO-L wave functions are presented in Figure 7. In each system, geometries of the $^2B_2$ and $^4B_2$ states are again very similar to each other. In going from DMX via DMX-N to DMX-P, the individual C−C bond distances within the upper carbon framework are changed, but the total length of the four C−C bonds is not significantly modified.

As seen in Table 3, the quartet−doublet energy gaps are small in both cases. For DMX-N, the MRMP2 method even suggests a reverse energy ordering. This result points out the importance of the intruder states effect (or otherwise the small denominator problem in the perturbation expansion), when treating quasi-degenerate states. Both calculations using MS-CASPT2 and intruder-state-free MCQDPT methods concur with each other, showing that the doublet $^2B_2$ state is marginally lower in energy, by 1.0 kcal/mol in DMX-N and 1.6 kcal/mol in DMX-P. We also assume that the corrections for ZPEs are small and do not modify the energy ordering. Therefore, this presents again a case of high-spin/low-spin quasidegenerate states with a small preference for the low-spin state.

Xylylene Triradical and Derivatives

J. Phys. Chem. A, Vol. 108, No. 40, 2004 **8417**

TABLE 3: Calculated Results Using MS-CASPT2/ANO-L, MRMP2/6-311G(d,p), and MCQDPT/6-311G(d,p) for DMX-N and DMX-P

state	main orbital configuration					active space[a]	total energy[b] (au) (relative energy in kcal/mol)		
	a1	a2	b2	b1	weight[c]		MS-CASPT2	MRMP2	MCQDPT
						DMX-N			
$^2B_2$	2u	2d0	2	22u00	0.603	(2315)	−340.149 97	−340.098 79	−340.096 50
	2u	2u0	2	22d00	0.203		(0)	(0)	(0)
	2u	2u0	2	2du0d	0.021				
	2u	dud	2	22u00	0.015				
	2u	2d0	2	2ud0u	0.013				
	2u	udu	2	22d00	0.013				
$^4B_2$	2u	2u0	2	22u00	0.819		−340.148 42	−340.099 03	−340.094 80
	2u	2d0	2	2uuu0	0.017		(1.0)	(−0.2)	(1.07)
	2u	udu	2	22u00	0.015				
						DMX-P			
$^2B_2$	2u	2d0	2	22u00	0.596	(2315)	−912.693 18	−912.562 77	−912.558 83
	2u	2u0	2	22d00	0.169		(0)	(0)	(0)
	2u	2u0	2	2dud0	0.026				
	2u	udu	2	22d00	0.018				
	2u	2d0	2	20u20	0.015				
	2u	2d0	2	2udu0	0.012				
	2u	dud	2	22u00	0.012				
	2u	2u0	2	2ddu0	0.011				
$^4B_2$	2u	2u0	2	22u00	0.778		−912.690 62	−912.560 19	−912.554 97
	2u	2d0	2	2uuu0	0.027		(1.6)	(1.6)	(2.4)
	2u	uuu	2	22d00	0.021				
	2u	2u0	2	20u20	0.015				
	2u	udu	2	22u00	0.011				

[a] Distribution of electrons in each of the C_{2v} symmetry representations. u and d stand for spin up and spin down, respectively. 2 stands for doubly occupied. [b] On the basis of CASSCF/ANO-L-optimized geometries given in Figure 7. [c] CI coefficients are obtained from CASSCF wave functions.

TABLE 4: Summary of Some Calculated Energetic Properties Related to the Triradicals

property	DMX	DMX-N	DMX-P
ΔE ($^4B_2-{}^2B_2$) (kcal/mol)	1.9	1.0	1.6
PA[a] (kcal/mol)	261	233	214
EA (eV)	1.1	2.3	4.95
IE (eV)	7.50	8.20	8.98
PA[a,b] (DMX$^-$) (kcal/mol)	401	367	371

[a] Using B3LYP and CCSD(T) calculations with the 6-311++G(3df,2p) basis set and corrected for ZPE. [b] Proton affinity of the corresponding anion.

In an attempt to obtain some useful thermochemical parameters for the triradicals considered, we have evaluated them using both CCSD(T) and B3LYP methods, and the results are tabulated in Table 4 which includes the doublet−quartet energy gap, the electron affinities, and proton affinities. It is worth noting that the EA of DMX tends to increase when going from CH to N and P. Similarly, the ionization energy of the MX biradical increases substantially in the same sequence. On the contrary, the PA of either the neutral DMX or the anion DMX$^-$ at the C5 site decreases significantly (by 20−30 kcal/mol). The PAs at other sites (N or P) have not been considered.

4. Concluding Remarks

In summary, in the present theoretical study, we have analyzed the electronic structure of the 5-dehydro-*meta*-xylylene (DMX) triradical and its two-nitrogen and two-phosphorus derivatives. Our quantum chemical computations lend support for the view that, in these triradicals, in which three electrons are being distributed in three open-shell $\sigma^1\pi^1\pi^1$ orbitals with comparable energies, the low-spin open-shell doublet state is slightly favored over the high-spin quartet state, even though the $^4B_2-{}^2B_2$ energy separation is small, amounting to, at most, 2 kcal/mol. This represents another case of a breakdown of the Aufbau principle of electron occupancy in molecular orbitals

and of Hund's rule. Some thermochemical parameters such as electron affinities, ionization energies, and proton affinities of the triradicals have also been evaluated. The calculated values agree well with experimental results where available.

Supporting Information Available: Molecular orbital diagrams and tables containing Cartesian coordinates. This material is available free of charge via the Internet at http://pubs.acs.org.

References and Notes

(1) (a) Salem, L.; Rowland, C. *Angew. Chem., Int. Ed. Engl.* **1972**, *11*, 92. (b) Wentrup, C. *Reactive Molecules*; Wiley: New York, 1984.

(2) Borden, W. T. Diradicals In *Encyclopedia of Computational Chemistry*; Schleyer, P. v. R., Ed.; Wiley: Chichester, U.K., 1999; Vol. 1, p 708.

(3) Wenthold, P. G.; Kim, J. B.; Lineberger, W. C. *J. Am. Chem. Soc.* **1997**, *119*, 1354.

(4) (a) Hrovat, D. A.; Borden, W. T. *THEOCHEM* **1997**, *398*, 211. (b) Fort, R. C.; Getty, S. J.; Hrovat, D. A.; Lahti, P. M.; Borden, W. T. *J. Am. Chem. Soc.* **1992**, *114*, 7549.

(5) Flock, M.; Pierloot, K.; Nguyen, M. T.; Vanquickenborne, L. G. *J. Phys. Chem. A* **2000**, *104*, 4022.

(6) Slipchenko, L. V.; Munsch, T. E.; Wenthold, P. G.; Krylov, A. I. *Angew. Chem., Int. Ed.* **2004**, *43*, 742.

(7) (a) Krylov, A. I. *Chem. Phys. Lett.* **2001**, *338*, 375. (b) Slipchenko, L. V.; Krylov, A. I. *J. Chem. Phys.* **2002**, *117*, 4694.

(8) (a) Hammad, L. A.; Wenthold, P. G. *J. Am. Chem. Soc.* **2001**, *123*, 12311. (b) Kemnitz, C. R.; Squires, R. R.; Borden, W. T. *J. Am. Chem. Soc.* **1997**, *119*, 6564.

(9) (a) Roos, B. O.; Taylor, P.; Siegbahn, P. A. E. *Chem. Phys.* **1980**, *48*, 157. (b) Ruedenberg, K.; Schmidt, M. W.; Gilbert, M. M.; Elbert, S. T. *Chem. Phys.* **1982**, *82*, 41.

(10) Anderson, K.; Malmqvist, P. A.; Roos, B. O. *J. Chem. Phys.* **1992**, *96*, 1218.

(11) Hirao, K. *Chem. Phys. Lett.* **1993**, *201*, 59; **1992**, *196*, 397; **1992**, *190*, 374.

(12) (a) Schmidt, M. W.; Gordon, M. S. *Annu. Rev. Phys. Chem.* **1998**, *49*, 233. (b) Witek, H. A.; Choe, Y. K.; Finley, J. P.; Hirao, K. *J. Comput. Chem.* **2002**, *23*, 957. (c) Schucan, T. H.; Weidenmuller, H. *Ann. Phys.* **1973**, *76*, 483; **1972**, *73*, 108.

(13) Brandow, B. H. *Rev. Mod. Phys.* **1967**, *39*, 771; *Int. J. Quantum Chem.* **1979**, *15*, 207.

(14) Finley, J. P.; Malmqvist, P. A.; Roos, B. O.; Serrano-Andres, L. *Chem. Phys. Lett.* **1998**, *288*, 299.

(15) Nakano, H. *J. Chem. Phys.* **1993**, *99*, 7983.

(16) Parr, R. G.; Yang, W. *Density Functional Theory of Atoms and Molecules*; Oxford University Press: New York, 1989.

(17) Frisch, M. J.; Trucks, G. W.; Schlegel, H. B.; Scuseria, G. E.; Robb, M. A.; Cheeseman, J. R.; Zakrzewski, V. G.; Montgomery, J. A., Jr.; Stratmann, R. E.; Burant, J. C.; Dapprich, S.; Millam, J. M.; Daniels, A. D.; Kudin, K. N.; Strain, M. C.; Farkas, O.; Tomasi, J.; Barone, V.; Cossi, M.; Cammi, R.; Mennucci, B.; Pomelli, C.; Adamo, C.; Clifford, S.; Ochterski, J.; Petersson, G. A.; Ayala, P. Y.; Cui, Q.; Morokuma, K.; Malick, D. K.; Rabuck, A. D.; Raghavachari, K.; Foresman, J. B.; Cioslowski, J.; Ortiz, J. V.; Stefanov, B. B.; Liu, G.; Liashenko, A.; Piskorz, P.; Komaromi, I.; Gomperts, R.; Martin, R. L.; Fox, D. J.; Keith, T.; Al-Laham, M. A.; Peng, C. Y.; Nanayakkara, A.; Gonzalez, C.; Challacombe, M.; Gill, P. M. W.; Johnson, B. G.; Chen, W.; Wong, M. W.; Andres, J. L.; Head-Gordon, M.; Replogle, E. S.; Pople, J. A. *Gaussian 98*, revision A.7; Gaussian, Inc.: Pittsburgh, PA, 1998.

(18) *GAMESS* program: Schmidt, M. W.; Baldridge, K. K.; Boatz, J. A.; Elbert, S. T.; Gordon, M. S.; Jensen, J. H.; Koseki, S.; Matsunaga, N.; Nguyen, K. A.; Su, S. J.; Windus, T. L.; Dupuis, M.; Montgomery, J. A. *J. Comput. Chem. Phys.* **1993**, *14*, 1347.

(19) Anderson, K.; Blomberg, M. R. A.; Fulscher, M. P.; Karlstrom, G.; Lindh, R.; Malmqvist, P. A.; Neogrady, P.; Olsen, J.; Roos, B. O.; Sadlej, A. J.; Schutz, M.; Seijo, L.; Serrano-Andreas, L.; Siegbahn, P. E. M.; Wildmark, P. O. *MOLCAS*, version 4; Lund University, Sweden.

(20) McWeeny, R. *Philos. Mag. B* **1994**, *69*, 727.

(21) Nguyen, M. T.; Zhang, R.; Nam, P. C.; Ceulemans, A. *J. Phys. Chem. A* **2004**, *108*, 6554 and references therein.

(22) Werner, H.-J. In *Ab Initio Methods in Quantum Chemistry, II*; Lawley, K. P., Ed.; John Wiley & Sons: New York, 1987; Vol. 69, p 1.